Anna C. Bakenecker*, Carlos Chinchilla and Thorsten M. Buzug*

Actuation of a magnetically coated swimmer in viscous media with a magnetic particle imaging scanner

Abstract: Magnetic actuation of medical devices is of great interest in improving minimally invasive surgery and enabling targeted drug delivery. With untethered, magnetically coated swimmers it is aimed at reaching regions of the body difficult to access with catheters. Such a swimmer was previously presented, which is suitable for the navigation by the magnetic fields of a magnetic particle imaging (MPI) scanner. The swimmer could be imaged with MPI as well, enabling the tomographic real-time tracking of the actuation process. In this work the steerability of the swimmer is further investigated in media of varying viscosities. For this, glycerol-water-mixtures of different mixing ratios were used. The velocities of the swimmer were measured for viscosities between those of pure glycerol and pure water. The experiments were performed with an MPI scanner at maximal magnetic field strength of the actuating fields. A viscosity range was found in which the swimmer is steerable by the fields of an MPI scanner, which leads to a prediction of the applicability of the swimmer in different body fluids.

Keywords: Magnetic actuation, magnetic manipulation, magnetic particle imaging, MPI, magnetic nanoparticles, magnetic swimmer

https://doi.org/10.1515/cdbme-2020-3090

1 Introduction

The actuation of medical devices with magnetic fields is under investigation. It enables the untethered steering of helically shaped swimmers providing the opportunity to reach areas of the body difficult to access. Hence, this technique has the potential to improve the precision of minimally invasive surgery, enables targeted drug delivery and has the potential to be used for local hyperthermia.

Swimmers of mm-size can be used for the navigation through the vascular system to reach pathological sites and deliver therapeutics [1-3]. The main challenges to be faced by those swimmers are the viscosity of blood, the pulsating blood pressure, and the navigation through an irregular vascular system.

For future in-vivo applications of magnetic actuation, a tomographic real-time tracking of the above described devices and swimmers is indispensable. Magnetic particle imaging (MPI) is a technique introduced as especially beneficial for the visualization of the actuation process [1,4-7]. An MPI scanner provides magnetic fields which cannot only be used for the visualization of magnetic nanoparticles, but also for magnetic actuation by using homogeneous rotating magnetic fields [1,6]. Therefore, an MPI scanner can be dually used for imaging and magnetic actuation. Since MPI images magnetic concentration distribution of magnetic nanoparticles, it allows for imaging the magnetically coated swimmers without any labelling. Further, MPI is a three-dimensional, real-time imaging technique, without ionizing radiation; hence MPI has a high potential for interventional and vascular imaging [8-10].

Usually, the aforementioned actuation devices were investigated in-vitro in water filled phantoms. However, the swimming performance needs to be investigated for viscous media, as performed by [2]. In this work the dynamic behaviour of the mm-sized swimmer introduced in [1] was further investigated experimentally and by numeric simulations in media of varying viscosities, in order to investigate in which biological fluids this swimmer can be deployed.

2 Theory

The focus fields of an MPI scanner are homogeneous magnetic fields, which are typically used to enlarge the field of view.

***Corresponding authors: Anna C. Bakenecker, Thorsten M. Buzug:** University of Lübeck, Institute of Medical Engineering, Ratzeburger Allee 160, 23562 Lübeck, Germany, e-mail: {Bakenecker,Buzug}@imt.uni-luebeck.de
Carlos Chinchilla: University of Lübeck, Institute of Medical Engineering, Lübeck, Germany

However, they can also be used for manipulation by applying sinusoidal currents to the three pairs of coils arranged in Helmholtz configuration. The strength is adjustable in all three spatial directions. A homogeneous magnetic field with a rotating field vector is generated, which has the form

$$\vec{\boldsymbol{B}}(\boldsymbol{t}) = \begin{pmatrix} \mathbf{0} \\ \pm \boldsymbol{B}\,\mathbf{sin}(\mathbf{2\pi}\boldsymbol{ft}) \\ \boldsymbol{B}\,\mathbf{cos}(\mathbf{2\pi}\boldsymbol{ft}) \end{pmatrix} \quad (1)$$

when a forward movement in x-direction is intended, the plane of rotation is in y/z. The "±" indicates a clockwise or counterclockwise rotation of the magnetic field vector. An object with a magnetic moment $\vec{m}$ aligns with an applied magnetic field. The magnetic torque reads

$$\vec{T} = \vec{m} \times \vec{B}. \quad (2)$$

If a homogeneous rotating magnetic field of the form (1) is applied, an object with the magnetic moment $\vec{m}$ follows the magnetic field and rotates around its x-axis. The forward movement of the magnetic object depends on the shape and the surrounding media. The latter can be described by the viscous drag force

$$F_{\mathrm{D}} = \frac{1}{2}\rho v^2 \mathrm{C_D} A, \quad (3)$$

where ρ denotes the density of the fluid, v the velocity of the object, $\mathrm{C_D}$ the drag coefficient, which depends on the objects' shape and A the cross section of the object. Further, the buoyancy of an object is important to describe its movement in viscous media:

$$F_{\mathrm{B}} = \rho \mathrm{g} V, \quad (4)$$

with g being the gravitational acceleration an V the object volume, assuming that the whole object is surrounded by the media. This force points in opposite direction as the gravitational force, hence the residual gravitational force acting on the swimmer is:

$$F_{\mathrm{G}} = m\mathrm{g} - \rho \mathrm{g} V. \quad (5)$$

3 Methods and Materials

In this section, the swimmer, the MPI scanner, as well as the velocity measurements in media of different viscosities, are being described.

3.1 The swimmer

A swimmer of 1.8 mm width and 4.5 mm length was used, which was previously presented in [1]. The swimmer has a helical Savonius shape and was coated with magnetic nanoparticles. The suitability of the swimmer visualizable with MPI was shown before.

3.2 Numeric simulations on the swimmer velocity in viscous media

Numeric simulations on the swimmer velocity were performed using COMSOL Multiphysics. The CAD model of the swimmer was imported into COMSOL from SolidWorks and placed in the middle of a water filled cylinder. Simulations were conducted for different viscosities at a rotation frequency of 10 Hz for 1 s using time steps of 0.01 s. The rotation frequency had to be ramped up within the first 0.3 s, before reaching the aimed rotation frequency.

3.3 The velocity measurements in viscous media

A preclinical MPI scanner (25/20FF, Bruker BioSpin MRI GmbH, Ettlingen, Germany) was used to perform the manipulation of the swimmer. The maximum focus field strength of 17.7 mT was applied according to equation (1) inducing a movement of the swimmer in the direction of the scanner bore with a rotation frequency of 10 Hz. The swimming velocity was measured for different viscosities of the surrounding media. A glycerol-water-mixture of varying volume fractions was used to realize viscosities between 1 mPa·s (water) and 1255 mPa·s (glycerol). The viscosity of the medium depends on the temperature and the mixing ratio. The temperature was measured before and after each measurement. Water was added to 4 ml glycerol to vary the viscosity. The viscosity was then calculated according to [11] by using the mean temperature, the water, and the glycerol volumes. Glycerol-water-mixtures of 23 different mixing ratios were filled one after the other into a 5 cm long glass cylinder of 1 cm diameter and 5 cm length. The magnetically

coated swimmer was inserted into the medium. The phantom was placed in the centre of the MPI scanner. An endoscopic camera with an attached mirror was placed below the phantom to record the movement of the swimmer. The rotating focus fields were applied four times for 5 s. Video stills before and after each moving sequence were used to read out the travelled distance at the scale bar. The velocity was then calculated by the mean of two times forward and two times backward movement of the simmer. One of the video stills, which shows the setup of the experiment, can be seen in Figure 1.

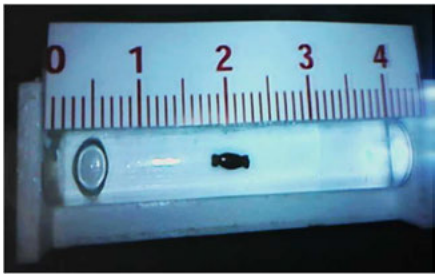

Figure 1: A video still of the swimmer inside the glass tube which is filled with a glycerol-water-mixture. The setup is positioned in the center of the MPI scanner bore. The camera position is below the setup. (The picture is mirrored here, because an endoscopic camera with an attached mirror was used for recording).

4 Results

The simulated swimmer velocity for different viscosities of the surrounding medium can be seen in Figure 2. A velocity of 7.8 mm/s was found in pure water. The velocity decreases for higher viscosities. The experimentally measured swimmer velocities as a function of the viscosity of the surrounding medium are shown in Figure 3. The swimmer did not move in the viscosity regime between 1255 mPa·s and 182 mPa·s. Between 83 mPa·s and 26 mPa·s the swimmer reacts to the magnetic field, but does not fulfil full rotation. The observed forward movement is a slip-stick motion. Between 22 mPa·s and 1 mPa·s, the swimmer showed full rotation and moved forward with a corkscrew like movement. The insert of Figure 3 shows this regime in detail, displaying an increasing velocity with increasing viscosity.

5 Discussion

The magnetic torque (2) has to overcome the viscous drag force (3), then the swimmer can fulfil full rotation. This occurs

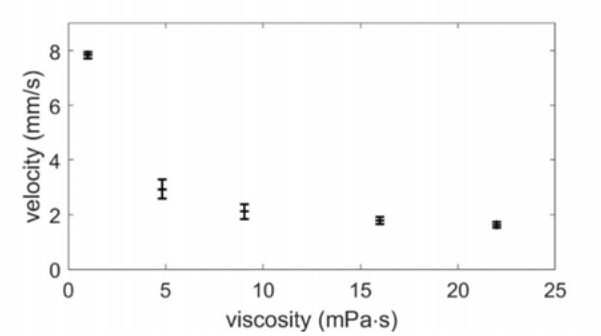

Figure 3: Numeric simulations of the swimmer velocity as a function of the viscosity of the medium. Displayed data points are the mean values of the data points, error bars indicate the standard deviation.

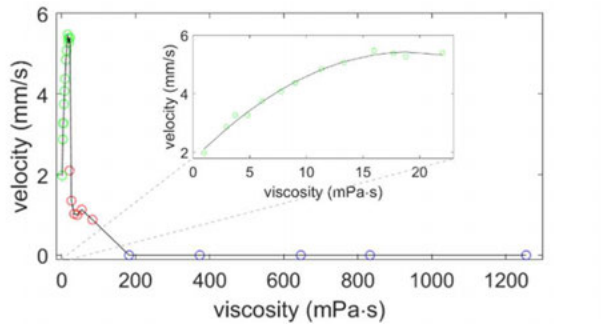

Figure 2: Velocity of the swimmer as a function of the viscosity of the medium. The measured velocities for the whole viscosity range between pure glycerol (1255 mPa·s) and pure water (1 mPa·s) is shown. The colors indicate no movement of the swimmer (blue), an uncertain sliding of the swimmer (red) and a straight forward movement of the swimmer due to full rotation (green). The insert shows this regime with a polynomial fit.

at viscosities between 26 mPa·s and 22 mPa·s. For smaller viscosities the magnetic torque is larger than the viscous drag force and the swimmer can fulfil full rotation and a corkscrew like forward movement. This regime was further investigated by numeric simulations. The simulations show a decreasing velocity with increasing viscosity, while the experimental results show an increasing velocity. One has to account for the buoyancy of the swimmer (4) and the resulting force acting on the swimmer (5), which decreases with increasing viscosity. This was not taken into account for the simulations. The swimmer lies on the bottom of the glass and experiences a frictional force. This depends on the residual gravitational force (5) acting on the swimmer. The more buoyant the swimmer, the less frictional force it experiences. That might be an explanation why the swimmer shows higher velocities for higher viscosities in the experimental results

In order to predict possible application areas, the findings can be compared with viscosities of different body fluids.

Since the size of the swimmer is suitable for the navigation through larger blood vessels the comparison with blood is obvious. At a body temperature of 37°C blood has a viscosity of about 4.5 times that of water [12]. (Water has a viscosity of 0.7 mPa·s at 37°C.) Therefore, it is expected that the swimmer is steerable in blood. However, the viscosity depends strongly on the haematocrit (volume percentage of red blood cells) as well as the vessel diameter the blood flows through. Further, blood is strictly speaking a non-Newtonian fluid, because of the red blood cells. Whereas water and glycerol are Newtonian fluids. The viscosity of urine is about 1.2 times that of water at body temperature [13]. It is expected that the swimmer is suitable for applications in the bladder. Mucus has a viscosity of about 2,000 times that of water [14]. Hence, it is not expected that the swimmer is able to be steered through mucus.

6 Conclusion

In this work, the velocity of a magnetically steerable swimmer was investigated for varying viscosities of the surrounding medium, experimentally and by numeric simulations. It was found that the magnetic force could not overcome the viscous drag force for viscosities larger than 22 mPa·s. It could be observed that the velocity of the swimmer increases with increasing viscosities for a viscosity range between 1 mPa·s and 22 mPa·s. The numeric simulations show a decreasing velocity in this regime. This is due to the buoyancy of the swimmer, which is larger for larger viscosities leading to a smaller frictional force between the swimmer and the phantom wall.

Future application scenarios for the swimmer are the transport of therapeutics through the vascular system for targeted drug delivery. The results of the here presented work indicate the applicability of the swimmer in different body fluids. It is expected that the magnetic torque generated by an MPI scanner is sufficiently high to steer the swimmer through blood. However, depending on the exact application area the pulsatile blood flow needs to be taken into account. It could be shown previously that this swimmer can be steered in different directions and can be visualized with MPI. This work further investigated the swimming behaviour in dependency of the viscosity of the surrounding medium and indicates the suitability of navigating the swimmer through blood and other body fluids.

Author Statement

Research funding: The authors gratefully acknowledge Federal Ministry of Education and Research, Germany (BMBF) for funding this project under Grant No. 13GW0230B (FMT). Conflict of interest: Authors state no conflict of interest. Informed consent: Informed consent has been obtained from all individuals included in this study. Ethical approval: The conduct research is not related to either human or animals use.

References

[1] A. C. Bakenecker, A. von Gladiss, T. Friedrich, U. Heinen, H. Lehr, K. Lüdtke-Buzug, and T. M. Buzug. Actuation and visualization of a magnetically coated swimmer with magnetic particle imaging. Journal of Magnetism and Magnetic Materials, (2018). doi: 10.1016/j.jmmm. 2018.10.056.

[2] H.-W. Huang, F. E. Uslu, P. Katsamba, E. Lauga, M. S. Sakar, B. J. Nelson. Adaptive locomotion of artificial microswimmers. Science Advances (2019): Vol. 5, no. 1, doi: 10.1126/sciadv.aau1532.

[3] K. Kikuchi ; A. Yamazaki ; M. Sendoh ; K. Ishiyama ; K.I. Arai, Fabrication of a spiral type magnetic micromachine for trailing a wire, IEEE Transactions on Magnetics 41 (10) (2005), doi: 10.1109/TMAG. 2005.855155

[4] J. Rahmer, D. Wirtz, C. Bontus, J. Borgert, B. Gleich, Interactive magnetic catheter steering with 3-d real-time feedback using multi-color magnetic particle imaging, IEEE Trans. Med. Imaging 36 (2017) 1449–1456, doi: 10.1109/TMI.2017.2679099.

[5] N. Nothnagel, J. Rahmer, B. Gleich, A. Halkola, T.M. Buzug, J. Borgert, Steering of magnetic devices with a magnetic particle imaging system, IEEE Trans. Biomed. Eng. 63 (11) (2016) 2286–2293, doi: 10.1109/TBME.2016.2524070.

[6] J. Rahmer, C. Stehning, B. Gleich, Spatially selective remote magnetic actuation of identical helical micromachines, Sci. Rob. 2 (3) (2017) 2845, doi: 10.1126/scirobotics.aal2845.

[7] J. Rahmer, C. Stehning, B. Gleich, Remote magnetic actuation using a clinical scale system, PLOS ONE 13 (3) (2018) e0193546, doi: 10.1371/journal.pone.0193546.

[8] B. Gleich, J. Weizenecker, Tomographic imaging using the nonlinear response of magnetic particles, Nature 435 (7046) (2005) 1214–1217, doi: 10.1038/nature03808

[9] J. Weizenecker, B. Gleich, J. Rahmer, H. Dahnke, J. Borgert. Three-dimensional real-time in vivo magnetic particle imaging. Phys Med Biol. (2009) Mar 7;54(5):L1-L10. doi: 10.1088/0031-9155/54/5/L01

[10] A. C. Bakenecker, M. Ahlborg, C. Debbeler, C. Kaethner, T. M. Buzug, and K. Lüdtke-Buzug. Magnetic particle imaging in vascular medicine, Innovative Surgical Sciences, 3, 179, (2018) doi: 10.1515/iss-2018-2026.

[11] N. S. Cheng, Formula for viscosity of glycerol-water mixture, Industrial and Engineering Chemistry Research, 47 (2008) 3285-3288, doi: 10.1021/ie071349z.

[12] H. Rein and M. Schneider, Physiologie des Menschen, Springer Verlag, (1956) 12th Edition, p. 105

[13] R. Burton-Opitz and R. Dinegar, The viscosity of urine, American Journal of Physiology-Legacy Content Volume 47, Issue 2 (1918) doi: 10.1152/ajplegacy.1918.47.2.220

[14] S. K. Lai, Y.-Y. Wang, D. Wirtz, and J. Hanes. Micro- and macrorheology of mucus. Adv Drug Deliv Rev. (2009) 61(2): 86–100. doi:10.1016/j.addr.2008.09.012.